Applied Science, Computing and Energy, 2026, 4(4), 632-646

Reservoir Characterization and the Quantitative Assessment of Hydrocarbon-Bearing Reservoir Sands in the Otodi Field, Niger Delta

Philip Asuquo Edem, Samuel Izama Ugar*, Selong Unanaonwi Edem, Dominic Akam Obi, Calvin Etongo Mbange, and Moses Ekene Obasi

Received: 19 February 2026/Accepted: 14 June 2026/Published: 20 June 2026

Abstract: *An integrated petrophysical and seismic reservoir characterization study was carried out in the Otodi Field, eastern Niger Delta, Nigeria, to evaluate reservoir quality and estimate hydrocarbon reserves. The study utilized a post-stack, time-migrated 3-D seismic volume (234 km²) together with wireline log suites, checkshot, and deviation data from four wells (KC1–KC4). Usable open-hole log suites (gamma ray, resistivity, density, sonic, neutron and caliper) were available for wells KC1–KC3, while KC4 was limited to checkshot data and was used only to support the regional time–depth framework. Petrophysical parameters such as shale volume, porosity, water saturation, hydrocarbon saturation, and permeability were computed in Petrel™ using standard empirical relationships (Schlumberger, 1974; Asquith & Krygowski, 2004; Hartman & Beaumont, 1999). Three hydrocarbon-bearing reservoir sands (I, II and III) were delineated. Porosity ranges from 19% to 28% (good to very good) and permeability from 60 mD to 477 mD (fair to very good), with hydrocarbon saturation ranging from 77% to 96%. Reservoirs I and III exhibit markedly better porosity and permeability character than reservoir II. Volumetric modelling yielded Stock Tank Oil Initially in Place (STOIIP) of 6,090 (×10³ bbl), 4,381 (×10³ bbl) and 5,658 (×10³ bbl) for reservoirs I, II and III. On this basis, reservoir I is the prospective hydrocarbon target in the field, followed by reservoir III, with reservoir II ranked as the least prospective of the three sands. Structurally, the field is dominated by a rollover-anticline trap style associated with NE–SW-trending listric growth faults, consistent with the regional structural style of the Niger Delta.*

Keywords: *Petrophysical analysis; porosity; permeability; reservoir characterization; reserve estimation; Niger Delta; 3-D seismic interpretation*

Philip Asuquo Edem
Department of Geology, University of Calabar, Calabar, Nigeria
Email: philipedem407@gmail.com
https://orcid.org/0009-0007-0509-5079

Samuel Izama Ugar*
Department of Geology, University of Calabar, Calabar, Cross River State, Nigeria
Email: samuelizama@yahoo.com

Selong Unanaonwi Edem
Department of Geology, University of Calabar, Calabar, Cross River State, Nigeria
Email: selonguedem@unical.edu.ng
https://orcid.org/0009-0008-5514-3355x

Dominic Akam Obi
Department of Geology, University of Calabar, Calabar, Cross River State, Nigeria
Email: dominic_odu@yahoo.com

Calvin Etongo Mbange
Department of Geology, University of Calabar, Calabar, Cross River State, Nigeria
Email: mbangecalvin81@gmail.com

Moses Ekene Obasi
Department of Geology, University of Calabar, Calabar, Cross River State, Nigeria
Email: me.obasi@gmail.com

1.0 Introduction

3-D seismic and well log data are among the most important subsurface datasets for characterising reservoir geometry and quality ahead of hydrocarbon development decisions. Hydrocarbon exploration and field development increasingly rely on integrated reservoir characterization to reduce geological uncertainty and optimize reservoir management. By combining seismic interpretation with petrophysical evaluation, reservoir characterization provides detailed information on

Also available @ https://doi.org/10.5281/zenodo.21701289

reservoir architecture, lithofacies distribution, fluid occurrence, reservoir continuity, and heterogeneity, thereby improving reserve estimation and production forecastingReservoir characterization involves the integration of geological, geophysical and petrophysical information to define reservoir geometry, lithology, fluid distribution and storage capacity. It combines extrinsic properties such as reservoir top and base, gross thickness, net-to-gross ratio, fluid contacts and net sand thickness with intrinsic properties including porosity, permeability, water saturation and hydrocarbon saturation to provide reliable estimates of hydrocarbon resources and reservoir performance. Petrophysics is the study of the physical properties of reservoir rocks and their contained fluids. Wireline log measurements provide the primary means of quantitatively determining reservoir properties such as shale volume, porosity, permeability and fluid saturation.

Petrophysical parameters in this study were computed from an integrated suite of caliper, sonic, gamma ray, resistivity, density and neutron logs, combined with checkshot data, using established empirical relationships (Schlumberger, 1974; Asquith & Krygowski, 2004; Hartman & Beaumont, 1999). These relationships were used to derive shale volume (Vsh), porosity (∅), water saturation (Sw), hydrocarbon saturation (Shc) and permeability (k). , Several studies have demonstrated the effectiveness of integrating seismic interpretation with well-log analysis for reservoir characterization in the Niger Delta. Evamy *et al*. (1978) established the structural framework of the Niger Delta petroleum province, while Doust and Omatsola (1989, 1990) described the relationship between growth faults, rollover anticlines and hydrocarbon accumulation. Emujakporue and Ngwueke (2013) showed that seismic structural interpretation significantly improves reservoir delineation, whereas Anthony *et al*. (2018) demonstrated that petrophysical evaluation provides reliable estimates of reservoir quality and hydrocarbon potential. More recently, Edem *et al*. (2026) highlighted the importance of integrating stratigraphic, seismic and facies analyses for identifying hydrocarbon traps within the Niger Delta.

Despite these advances, comparatively little information is available on the integrated reservoir characterization of the Otodi Field. Existing studies have largely focused on regional structural styles or neighbouring hydrocarbon fields, leaving uncertainties regarding reservoir continuity, petrophysical heterogeneity and hydrocarbon reserve distribution within the Otodi Field. Consequently, an integrated interpretation combining three-dimensional seismic data with comprehensive well-log analysis is required to improve reservoir evaluation and provide more reliable estimates of hydrocarbon resources.

This study provides an integrated workflow for evaluating reservoir quality, structural trapping mechanisms and hydrocarbon reserves in the eastern Niger Delta. The results will contribute to improved reserve estimation, field development planning and production optimization while providing a practical framework for reservoir characterization in similar deltaic hydrocarbon systems.

The aim of this study is to characterize the hydrocarbon-bearing reservoir sands of the Otodi Field and quantitatively estimate their hydrocarbon reserves through the integrated interpretation of three-dimensional seismic and well-log data.. The specific objectives are to:

(i) map the fault and horizon geometry of the field from 3-D seismic data and establish its structural trapping style;
(ii) delineate and correlate reservoir sand bodies across the available wells using gamma ray and resistivity log signatures;
(iii) compute the key petrophysical parameters (Vsh, porosity, water and hydrocarbon saturation, permeability) for each identified reservoir sand;
(iv) rank the identified reservoirs by hydrocarbon prospectivity; and
(v) estimate the Stock Tank Oil Initially in Place (STOIIP) for each reservoir sand using a Petrel-based volumetric workflow.

1.1 Geology of the Study Area

The Otodi Field is located within the eastern depobelt of the prolific Niger Delta Basin, one of the world's major hydrocarbon provinces. The basin contains numerous structurally and stratigraphically trapped hydrocarbon accumulations hosted primarily within the Agbada

Formation, making it an ideal setting for integrated reservoir characterization studies.

The Niger Delta extends over an area of more than 70,000 km² and comprises a regressive clastic sequence 9,000–12,000 m thick (Evamy *et al*., 1978; Emujakporue & Ngwueke, 2013). It is a large arcuate, tertiary, prograding sedimentary complex whose origin is linked to the rifting episode that separated Africa from South America (Tuttle *et al*., 1999). Five major depobelts are recognized, each with its own sedimentation, deformation and petroleum history: the Northern Delta, Greater Ughelli, Central Swamp, Coastal Swamp, and Offshore depobelts (Short & Stauble, 1967; Doust & Omatsola, 1990; Nwajide, 2013).

Well sections in the study area (Fig. 1) display the three classic lithostratigraphic subdivisions of the Niger Delta; the continental, shallow-marine, massive sand sequence approximately 200 m thick (Benin Formation), the coastal-marine sequence of alternating sands and shales, about 3,700 m thick, (Agbada Formation). This sand units form the principal producing reservoirs, with hydrocarbons trapped in rollover anticlines associated with growth faults (Doust & Omatsola, 1989; Onyia *et al*., 2002); and the basal marine shale unit estimated at 21,000 ft thick (Akata Formation)

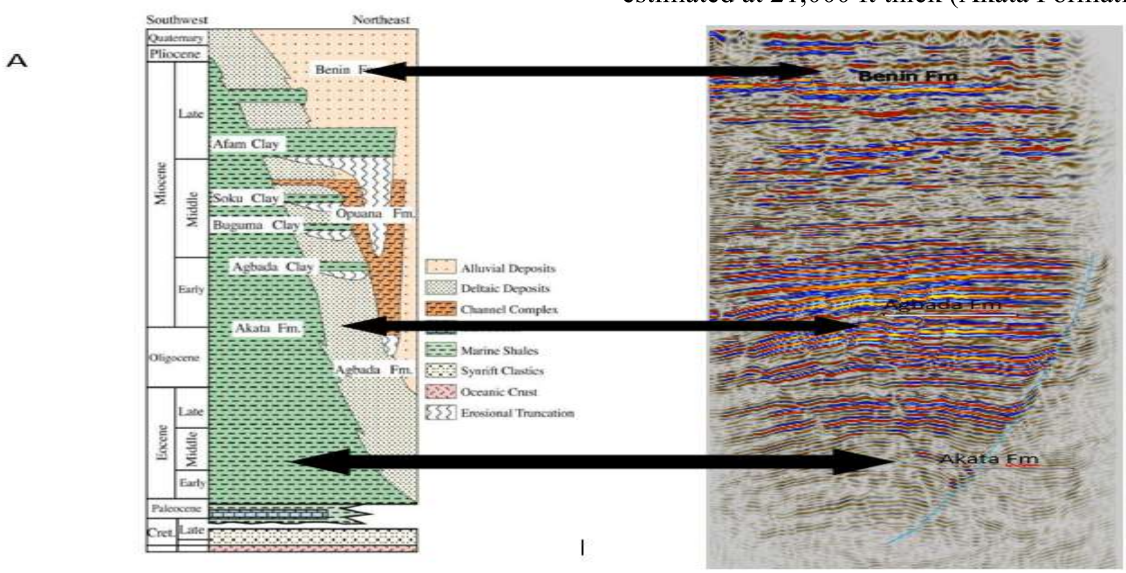

Fig. 1. Stratigraphic column in the field area showing the Benin, Agbada and Akata formations (Edem, *et al*., 2026)

The ratio of sedimentation rate to subsidence rate is the primary control on structural style, both regionally and at field scale. Recognized structural styles (Fig. 2) include simple non-faulted rollover anticlines, faulted rollover anticlines with multiple growth faults, complicated collapse-crest structures, k-block structures (sub-parallel growth faults), and structural closures along the back of major growth faults (Evamy *et al*., 1978). Normal faults, triggered by the movement of deep-seated, overpressured, ductile marine shale, have deformed much of the Niger Delta clastic wedge (Doust & Omatsola, 1989); many of these faults are syndepositional and affected sediment dispersal during delta progradation. These structural elements exert strong control on reservoir compartmentalization, hydrocarbon migration pathways and trap formation. Consequently, understanding their geometry and spatial distribution is fundamental for accurate reservoir characterization and reserve estimation in the Otodi Field.

2.0 Materials and Methods

The datasets used in this study were provided by a multinational petroleum operator in Nigeria and consisted of a post-stack, time-migrated three-dimensional (3-D) seismic volume, wireline log suites, checkshot surveys, and well deviation data. Data processing, seismic interpretation, petrophysical analysis, structural modelling, and volumetric reserve estimation were carried out using Schlumberger Petrel™ 2014. The seismic dataset is a post-stack, time-migrated 3-D volume covering 234 km², with inline and crossline lengths of 11 km and 21.3 km respectively, and a vertical trace length of six seconds. The survey comprises 852 N–S-oriented inlines and 441 E–W-oriented crosslines, both spaced at 25 m intervals, supplied in ZGY bricked format with variable-density display. The survey is zero-phase with SEG normal polarity, such that a positive increase in acoustic impedance is represented as a red peak.

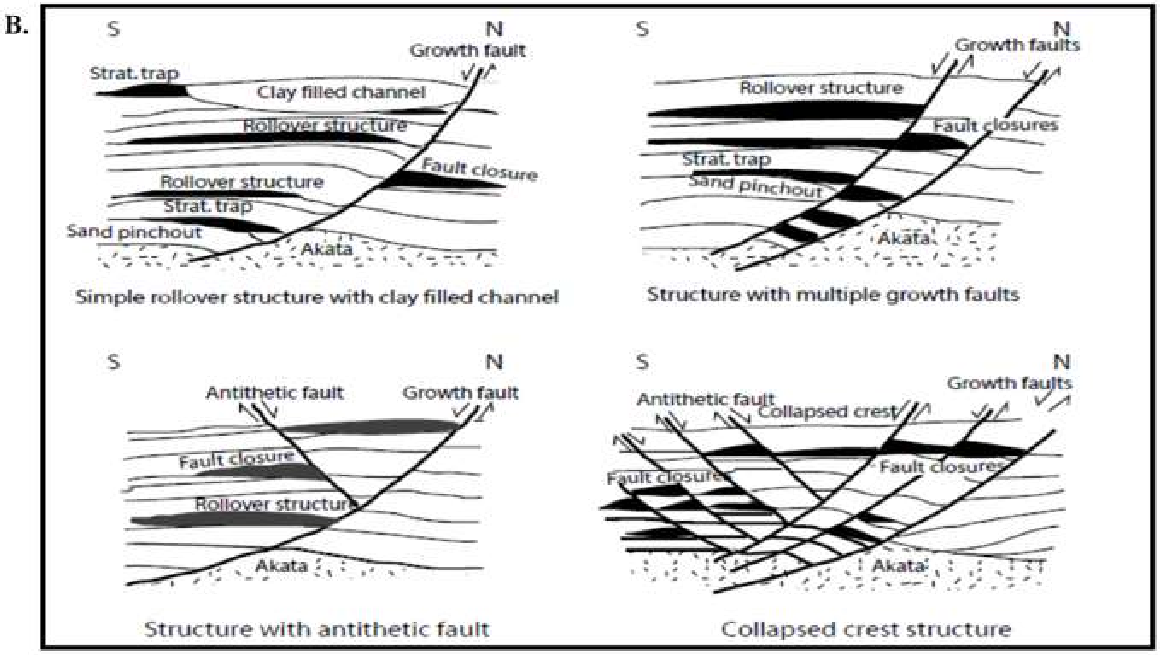

Fig. 2. Representative field-scale structural trap styles in the Niger Delta, analogous to the rollover-anticline geometry mapped in the Otodi Field (Evamy *et al*., 1978)

2.1 Well Data

Wireline log data were available from four wells KC1, KC2, KC3 and KC4 (Table 1) and were represented in grid (Fig. 3) within the study area. Complete open-hole log suites (gamma ray, resistivity, density, sonic and caliper) were available for KC1–KC3, enabling full petrophysical evaluation of these wells. KC4 was limited to checkshot data only and could not be petrophysically evaluated; it was retained solely to constrain the regional time–depth relationship used in the seismic-to-well tie. Prior to interpretation, the wireline logs were subjected to quality control, including depth matching, environmental correction where applicable, and inspection for washouts using caliper logs to ensure the reliability of the petrophysical analysis. This distinction resolves an apparent discrepancy in the original dataset description between "three wells" (used for petrophysical evaluation) and "four wells" (used across the full study, including seismic calibration).

Lithostratigraphic correlation of sand bodies within the Agbada Formation was carried out using gamma ray and resistivity logs, using a gamma-ray shale cut-off of **65 API**, selected based on the observed log response within the study area to distinguish clean reservoir sands from shale intervals.. Hydrocarbon-bearing sand bodies were identified from the combination of low gamma ray response and elevated resistivity. Horizons were mapped on the 3-D seismic volume to generate time and depth structure maps and to assess the role of faults as hydrocarbon migration pathways, followed by construction of a fault model to establish fault trends across the field.

Fault interpretation was carried out by tracking reflector discontinuities and fault throws across adjacent inlines and crosslines, while horizon interpretation involved continuous picking of key stratigraphic reflectors corresponding to the identified reservoir tops. Structural maps generated from the interpreted horizons were subsequently converted from time to depth using checkshot-derived velocity information. Seismic-to-well tie was performed using synthetic seismograms generated from sonic and density log data. Of the available wells, only KC1 and KC3 possessed both sonic and density logs required for synthetic seismogram generation (Table 1).

Table 1. Summary of wireline log suites available for each well (KC1–KC4) in the Otodi Field study area

Wells / Logs	KC1	KC2	KC3	KC4
Caliper	✓	✓	✓	×
Density	✓	✓	✓	×
Neutron	×	×	✓	×
Sonic	✓	×	✓	×
Gamma ray	✓	✓	✓	×
Resistivity	✓	✓	✓	×
Checkshot	×	✓	✓	×

× **= available; = not available.**

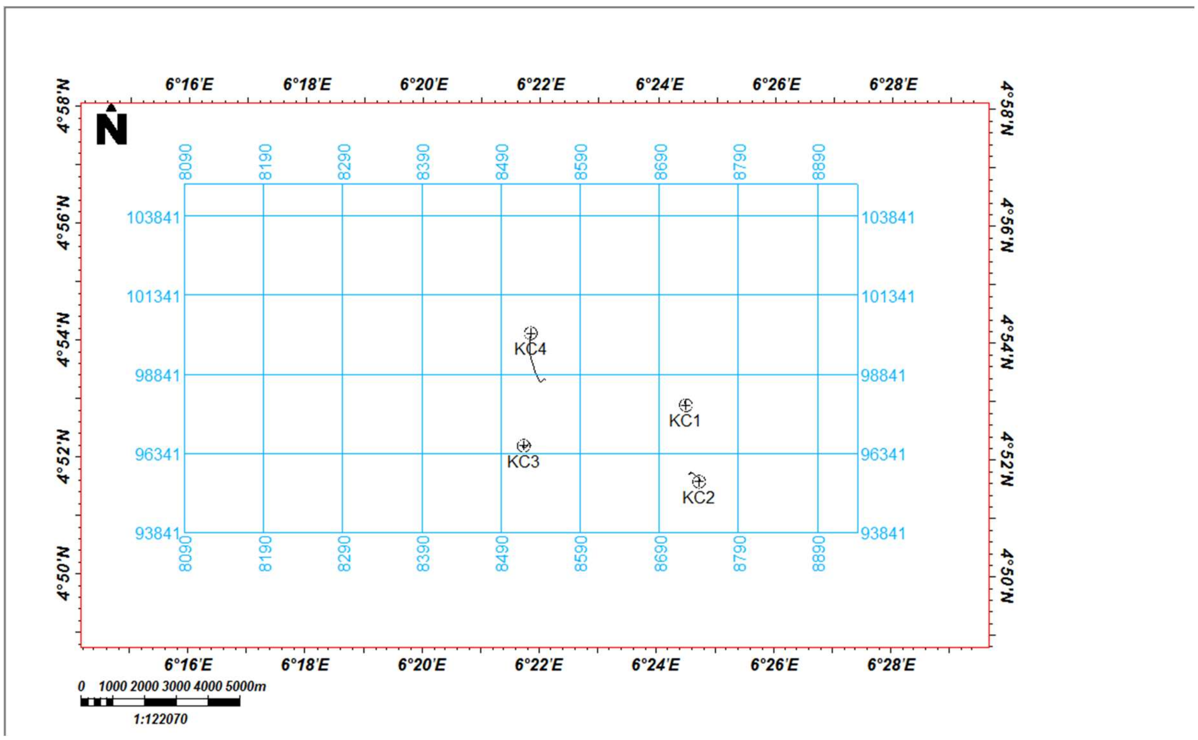

Fig. 3. Grid representation of the study area showing well locations (KC1–KC4). Vertical lines represent inlines (8090–8941); horizontal lines represent crosslines (93841–104841)

Consequently, the seismic-to-well tie was performed using these two wells.(Table 1); the synthetic seismograms shown in Figs. 9 and 10 therefore correspond to Wells KC1 and KC3. Reflectivity coefficients were computed from acoustic impedance contrasts and convolved with a 25 Hz zero-phase wavelet; a bulk shift of 2 milliseconds was applied to optimize the tie between the synthetic and the seismic traces. The quality of the seismic-to-well tie was assessed visually by matching major reflection events with the synthetic traces generated from the corresponding acoustic impedance logs.

2.2 Petrophysical Equations

Shale volume, porosity, water saturation and hydrocarbon saturation were computed using the following standard empirical relationships. Petrophysical properties were computed from standard industry equations widely applied in reservoir evaluation.

Gamma ray index:

$$IGR = \left(\frac{GR_{\log} - GR_{mix}}{GR_{\max} - GR_{min}}\right) \quad (1)$$

where GR_{log} is the gamma ray log reading of the formation, GR_{min} is the sand (clean) baseline, and GR_{max} is the shale baseline.

Linear shale volume (general form):

Vsh (linear) = IGR (2)

(2)

Shale volume for tertiary reservoirs

$$V_{sh} = 0.083 \times \left[2^{(3.7 \times IGR)} - 1\right] \quad (3)$$

Density-derived porosity (Asquith & Krygowski, 2004):

$$\emptyset D = \left(\frac{\rho_{ma} - \rho_b}{\rho_{ma} - \rho_l}\right) \quad (4)$$

where ØD is density-derived porosity, ρma is matrix density, ρb is the log-derived bulk density reading, and ρ_f is fluid density.

Sonic-derived porosity (Wyllie time-average equation):

$$\emptyset D = \left(\frac{\Delta_t - \Delta_{ma}}{\Delta_{tf} - \Delta_{tmax}}\right) \quad (5)$$

where Δ_t is the interval transit time of the formation, Δ_{tma} is the interval transit time of the matrix, and Δ_{tf} is the interval transit time of the formation fluid.

Density–neutron combined porosity (Hartman & Beaumont, 1999):

$$\emptyset ND = \sqrt{\left[\left(\frac{\emptyset N^2 + \emptyset D^2}{2}\right)\right]} \quad (6)$$

This formulation is sensitive to gas effect (crossover): when gas is present, neutron porosity reads lower than density porosity, whereas in wet sands the two curves converge. Neutron and density logs were shale-corrected prior to combination, and effective porosity was derived by subtracting the shale-fraction porosity from total porosity, following the Vsh log.

Water saturation was computed using the Archie equation calibrated with formation water resistivity derived from the resistivity logs in the clean, water-bearing intervals, and hydrocarbon saturation was obtained as Shc = 1 − Sw. Permeability was estimated from porosity–permeability transforms calibrated against the Levorsen (1967) qualitative classification (Table 2).

3.0 Results and Discussion

3.1 Fault and Horizon Interpretation

Faults were mapped on seismic inlines at 10-trace intervals (Fig. 4), identified from observable fault throw, discontinuous reflector geometry, and amplitude distortion within fault zones. The predominance of growth faults and rollover anticlines confirms that structural deformation associated with syn-sedimentary fault movement exerted significant control on hydrocarbon migration and trapping within the Otodi Field. This structural style is consistent with the regional tectonic framework of the Niger Delta described by Evamy *et al*. (1978) and Doust and Omatsola (1989), where listric growth faults generate structural closures favourable for hydrocarbon accumulation.

Mapped faults trend broadly East–West, with closely to sub-parallel faults forming a k-block structure in the northeast and a collapse-crest feature in the northwest and north-central parts of the study area. Growth faults in the central part of the field exhibit good closure and are capable of trapping hydrocarbon due to favourable fault intersections, whereas faults in the northern part lack such intersections and are non-trapping. In the seismic-to-well tie, the top of each reservoir was found to correspond to the crest (peak) of the reflection amplitude, and the base to the corresponding trough. The observed structural configuration suggests that hydrocarbon prospectivity is greatest within the central structural closures, where fault-assisted migration pathways coincide with effective structural traps. Such structural compartmentalization is characteristic of many productive reservoirs in the Agbada Formation.

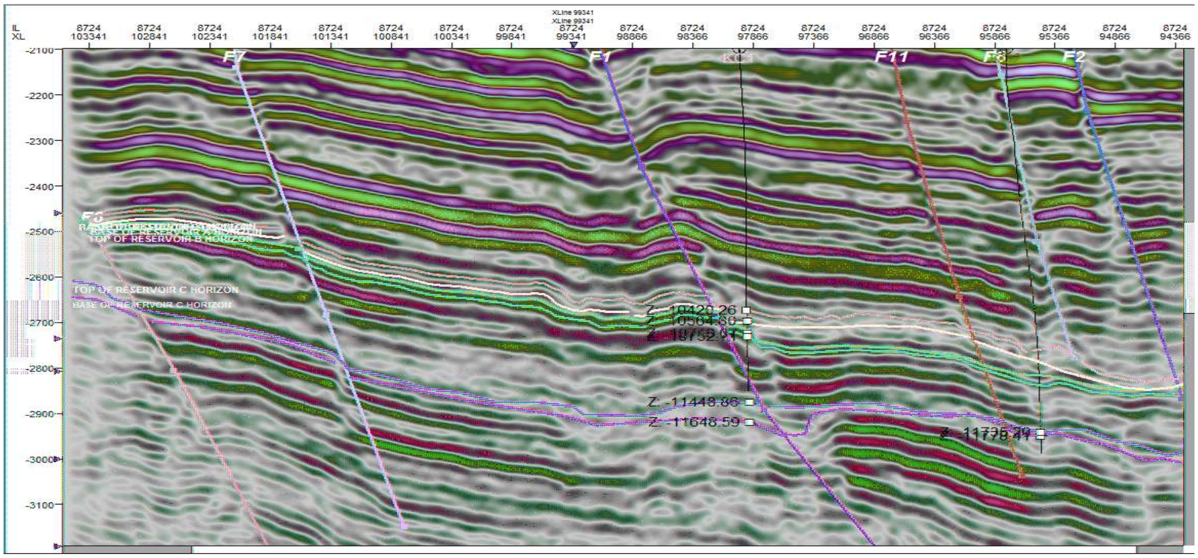

Fig. 4. Seismic inline section showing mapped faults (black polygons) and interpreted reservoir horizons across the Otodi Field study area.

3.2 Well Log Interpretation and Correlation

Log character from each well was used to classify lithological units, which were then correlated across the wells using gamma ray and resistivity signatures (Fig. 5). Three reservoir sands I, II and III were delineated. Reservoir sand III was correlated across KC1, KC2 and KC3; reservoirs A and B were identified only in KC01, as the corresponding intervals in KC2 and KC03 did not present equivalent clean-sand signatures during correlation (rather than being absent from the dataset). No reservoir sand could be evaluated in KC4 owing to the absence of open-hole log data in that well (Table 1).

Correlation of these reservoirs across the wells indicates lateral continuity of the principal hydrocarbon-bearing sand bodies, although variations in thickness and log response suggest localized depositional heterogeneity and structural compartmentalization. Such heterogeneity is typical of fluvio-deltaic reservoirs within the Agbada Formation.

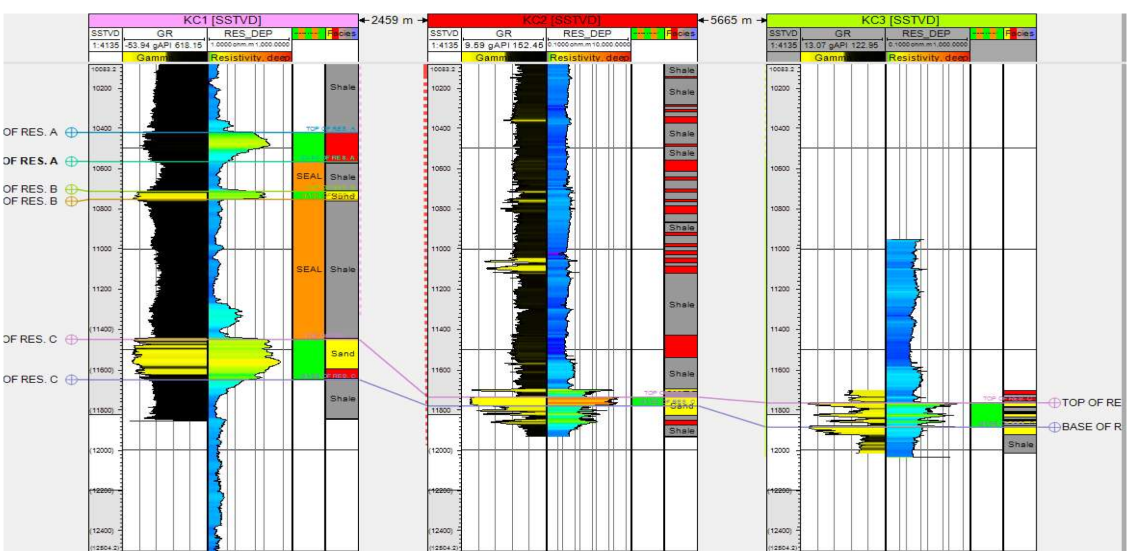

Fig. 5. Lithologic correlation of reservoir C across wells KC1, KC2 and KC3, based on gamma ray and resistivity log signatures

Gamma ray and resistivity signatures indicate that reservoir sands I, II and IIIare clean, hydrocarbon-bearing sands. Reservoir tops were picked at the deflection of the gamma ray log from shale into sand, with the reverse deflection used to pick the reservoir base. The consistent log signatures observed across the correlated wells demonstrate that gamma-ray and resistivity logs remain reliable indicators for distinguishing clean reservoir sands from surrounding shale units within the study area.Reservoir thickness distribution across the field is shown in Figs. 6a–c for reservoir sands I, II and III respectively, while the corresponding top and base picks used to define these intervals are illustrated in Fig. 7.

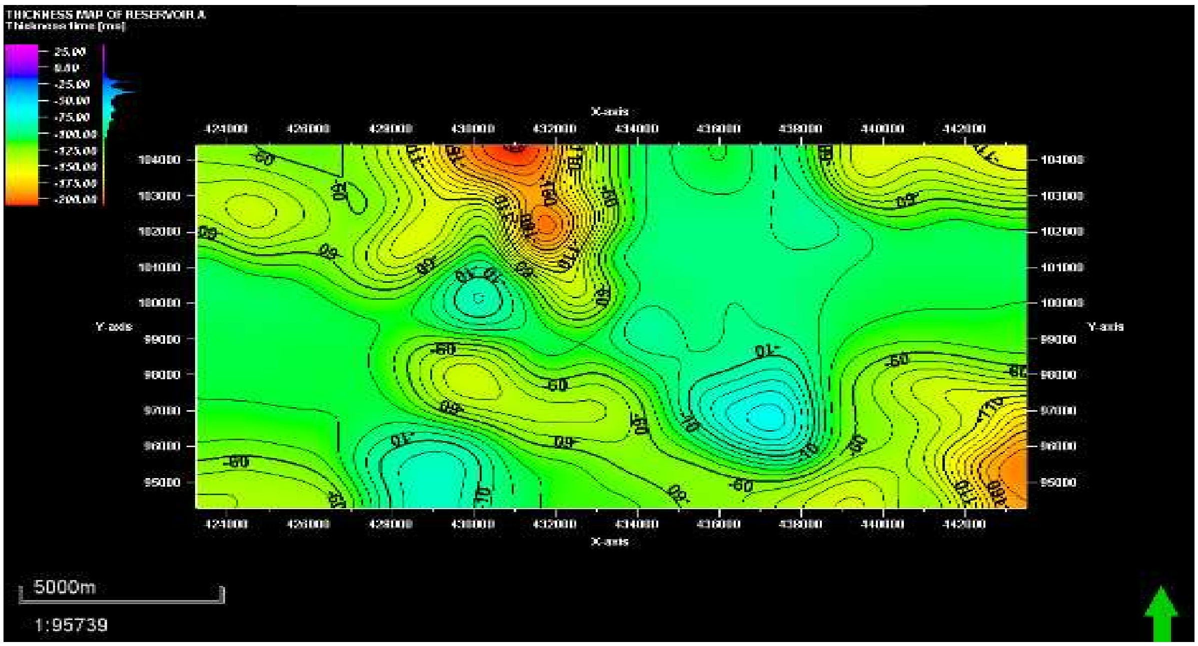

Fig. 6a. Isochron (two-way time) thickness map of reservoir sand I, contoured from the mapped top and base horizons

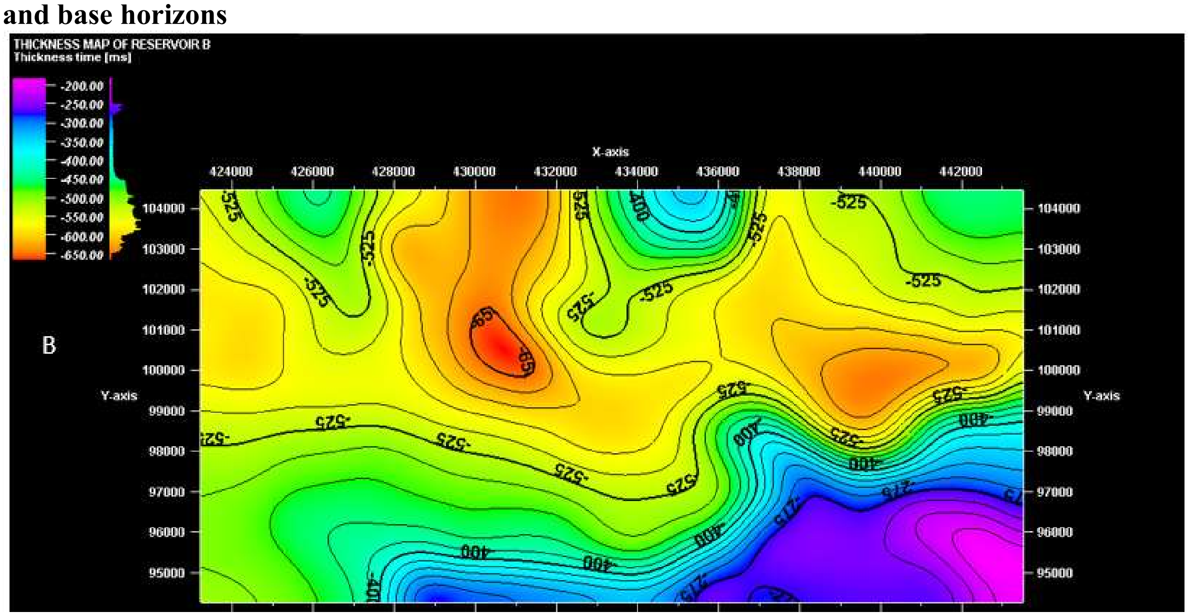

Fig. 6b. Isochron (two-way time) thickness map of reservoir sand II, contoured from the mapped top and base horizons

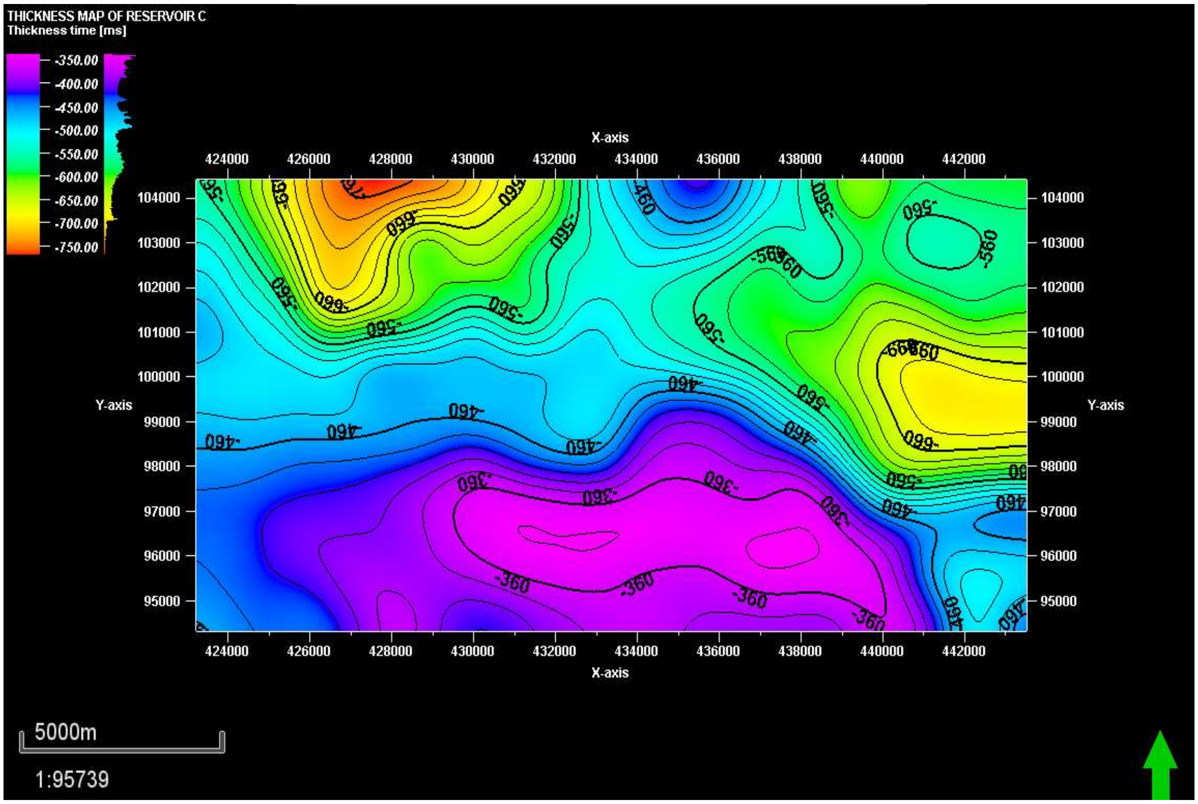

Fig/ 6c. Isochron (two-way time) thickness map of reservoir sand III, contoured from the mapped top and base horizons

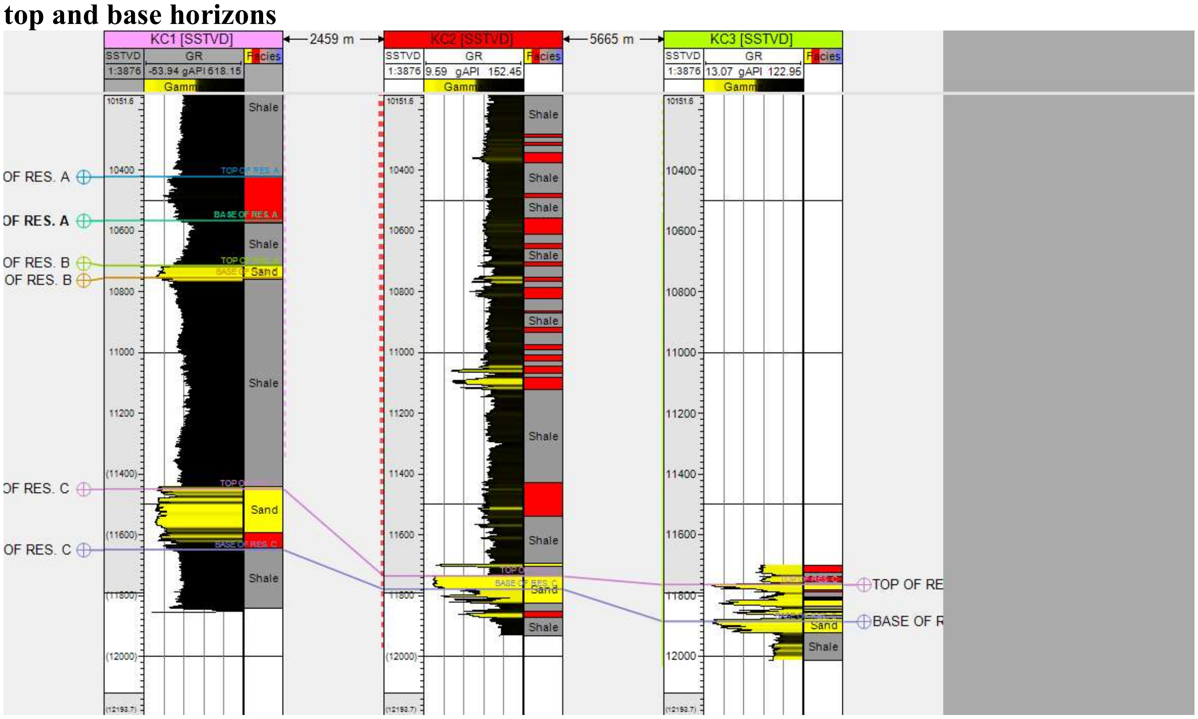

Fig. 7: Reservoir top and base picks identified from the gamma ray log for wells KC1, KC2 and KC3

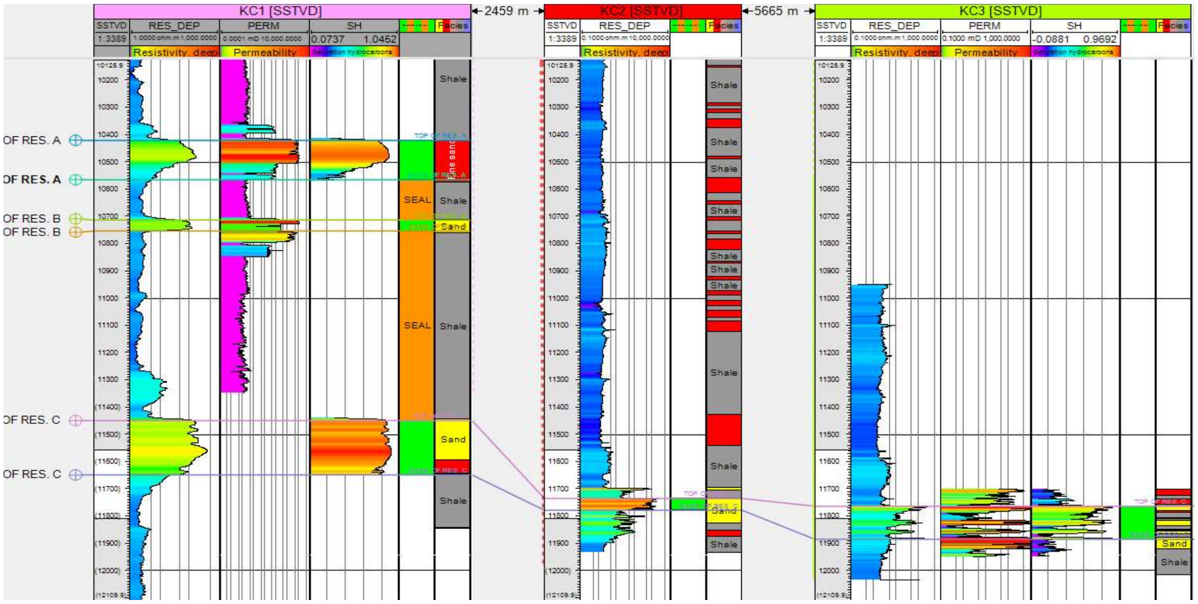

Fig. 8: Reservoirs I, II and III identified using gamma ray and resistivity log signatures across wells KC1, KC2 and KC3

3.3 Seismic-to-Well Tie

Because wells are recorded in depth and seismic data in time, a synthetic seismogram was generated for Wells KC1 and KC3 — the only wells with the sonic-and-density log pairing required for this step — to tie well-based reservoir picks to the seismic section. Reservoir tops and bases matched the peaks and troughs of the synthetic seismogram closely, confirming that the reservoir intervals were correctly identified on the wells.

The close agreement between the synthetic seismograms and seismic reflections demonstrates the reliability of the interpreted time-depth relationship and increases confidence in the mapped reservoir horizons. Accurate seismic-to-well calibration is essential for minimizing structural uncertainty during depth conversion and volumetric reserve estimation.

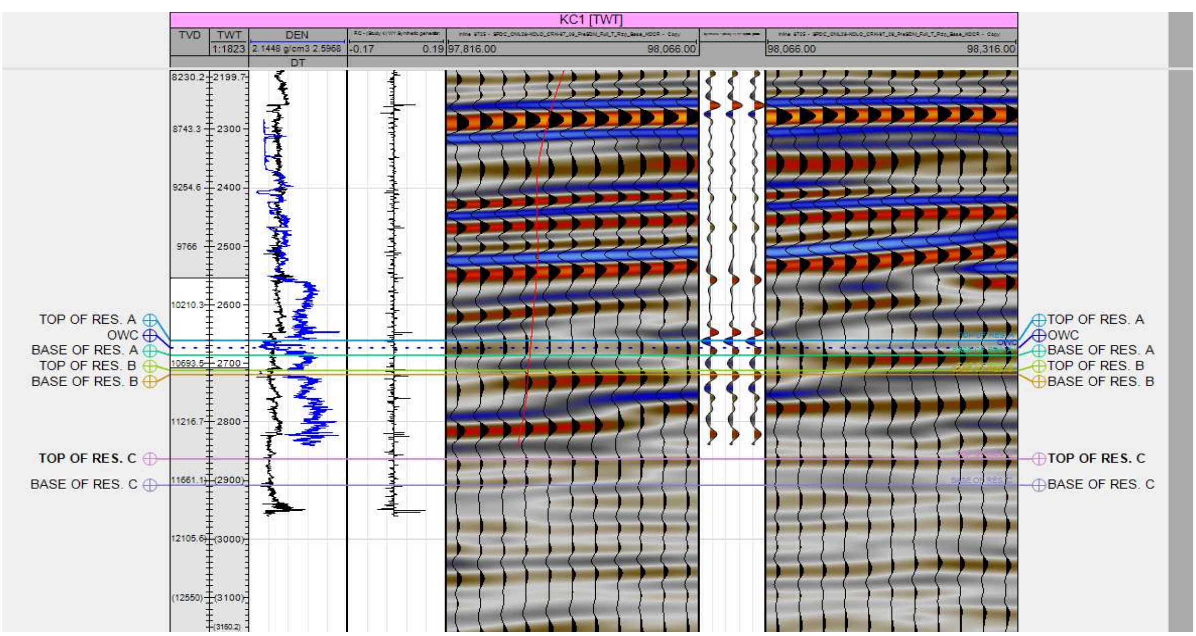

Fig. 9: Synthetic seismogram for Well KC1, used to tie reservoir tops and bases to the seismic section.

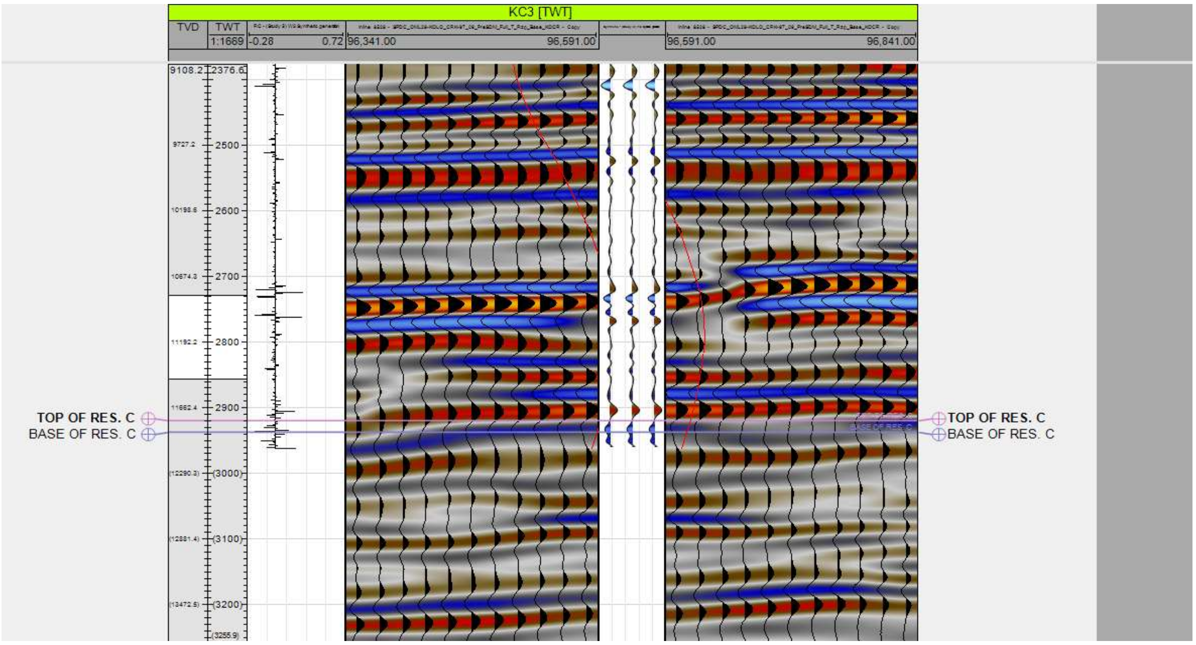

Fig. 10: Synthetic seismogram for Well KC3, used to tie reservoir tops and bases to the seismic section.

3.4 Petrophysical Results

Petrophysical logs for KC1–KC3 (Fig. 8) indicate that reservoir sands I, II and III are hydrocarbon-saturated, clean sands with minor thin-shale intercalation, evidenced by low gamma ray response. Reservoir I exhibits the most favourable petrophysical characteristics, combining high porosity, excellent permeability, low shale volume and high hydrocarbon saturation. These characteristics indicate superior reservoir quality and suggest that reservoir I possesses greater storage capacity and fluid transmissibility than reservoirs II and III. Neutron–density log character indicates the hydrocarbon phase is oil. It is only reservoir C that could be evaluated across the three Wells; KC1, KC2 and KC3. Reservoir III in Well KC2 shows high porosity but low permeability; but in Well KC3, it shows both high porosity and high permeability. Grain sorting and shape, packing style, depositional rate, matrix content, cementation, post-depositional compaction, and sand-to-shale ratio influence porosity in clastic systems (Anthony *et al*., 2018). The variation in permeability observed among the wells, despite comparable porosity values, suggests that permeability is controlled not only by pore volume but also by factors such as grain sorting, cementation, pore-throat geometry and diagenetic alteration. This observation agrees with Anthony *et al*. (2018), who reported that reservoir quality within the Niger Delta is strongly influenced by depositional and post-depositional processes. Table 2 presents the qualitative porosity/permeability classification (after Levorsen, 1967) used to grade the reservoirs in this study; Tables 3 and 4 summarize the extrinsic and intrinsic petrophysical parameters.

Table 2: Qualitative porosity and permeability classification scheme used to grade reservoir quality (after Levorsen, 1967)

Porosity (%)	Qualitative evaluation	Permeability (mD)	Qualitative evaluation
< 5	Negligible	< 1	Poor
5 – 10	Poor	1 – 15	Fair
10 – 15	Fair	15 – 50	Moderate
15 – 20	Good	50 – 250	Good
20 – 25	Very good	> 250	Very good

Table 3. Extrinsic reservoir parameters; top, base, fluid type, oil–water contact, gross thickness, net-to-gross and net sand for reservoirs I, II and III in well KC01, and reservoir sand III in wells KC02 and KC03

Sand / Well	Res. Top (ft)	Res. Base (ft)	Fluid Type	OWC (ft, SSTVD)	Gross Thk. (ft)	NTG (%)	Net Sand (ft)
I– KC01	10,420	10,564	Oil & Water	10,491	144	84	120.96
II – KC01	10,713	10,753	ODT	n/a	40	99	39.60
III – KC01	11,763	11,923	Oil & Water	11,581	202	39	78.78
III– KC02	11,735	11,871	–	11,769	136	30	40.80
III– KC03	11,763	11,923	–	11,863	160	30	48.00
A, B – KC02/KC03	n/e	n/e	n/e	n/e	n/e	n/e	n/e

****n/a = not applicable (ODT: oil-down-to, no defined OWC within logged interval); n/e = not encountered / not correlatable in this well. NTG is expressed here as a percentage (net sand ÷ gross thickness × 100), correcting a fraction/percentage labelling inconsistency present in the original dataset.**

Table 4. Intrinsic petrophysical properties — porosity, permeability, water saturation and hydrocarbon saturation — of the identified reservoirs by well

Sand	Well	Ø (%)	k (mD)	Sw (%)	Sh (%)
I	KC01	28	477.13	23	77
II	KC01	27	70	4	96
III	KC01	19	60	10	90
III	KC02	19	85	40	60
III	KC03	21	269	41	59

Reservoir I consistently demonstrates superior reservoir quality, with porosity of 28% and permeability exceeding 470 mD. Reservoir II exhibits similarly high porosity but considerably lower permeability, suggesting poorer pore connectivity despite favourable storage capacity. Reservoir III displays greater spatial variability between wells, reflecting reservoir heterogeneity.Based on the Levorsen (1967) classification, all evaluated reservoirs possess good to very good porosity, while permeability ranges from good to very good. These results indicate that the reservoirs are capable of supporting commercial hydrocarbon production, particularly reservoir I, which exhibits the highest permeability and hydrocarbon saturation.

3.5 Reserve Estimation

eserve estimation used the structural and property models of each reservoir, together with the interpreted oil–water contact, in a Petrel model-based volumetric workflow to compute the Stock Tank Oil Initially in Place (STOIIP) as presented in Table 5.

The volumetric analysis demonstrates that reservoir I contains the largest hydrocarbon volume, with an estimated STOIIP of 6.09×10^6 bbl, followed by reservoir III. The combination of high porosity, excellent permeability and large hydrocarbon pore volume makes reservoir I the most economically attractive target for future field development. Reservoir II, despite exhibiting relatively high porosity, contains the smallest hydrocarbon volume owing to its comparatively limited reservoir thickness and permeability. The ranking of reservoir prospectivity agrees with the petrophysical evaluation, confirming that permeability and effective reservoir thickness exert a stronger influence on reserve potential than porosity alone. Reservoir II, despite having favourable porosity, is limited by comparatively low permeability and the smallest reserve volume, and is therefore ranked as the least prospective of the three reservoirs.

Table 5. Petrel model-based volumetric results (GRV, net volume, pore volume, HCPV, STOIIP and recoverable oil) for reservoir sands I, II and III

Reservoir sand	GRV ($\times 10^6$ ft^3)	Net Volume ($\times 10^6$ ft^3)	Pore Volume ($\times 10^6$ ft^3)	HCPV ($\times 10^6$ rb)	STOIIP ($\times 10^3$ bbl)	RECOVERABLE OIL ($\times 10^3$ bbl)
I	34,202	34,202	6,090	6,090	6,090	2,436
II	19,732	19732	4,381	4,381	4,381	1,752
III	31,773	31,773	5,658	5,658	5,658	2,263

4.0 Conclusion

Integration of 3-D seismic and well log data in the Otodi Field identified three hydrocarbon-bearing reservoir sands (I, II and III) hosted within clean, good-quality sandstones of the Agbada Formation. Porosity ranges from 19% to 28% and permeability from 60 mD to 477 mD, both classed as good to very good; hydrocarbon saturation ranges from 77% to 96%. The structural style of the field is dominated by rollover anticlines associated with NE–SW-trending listric growth faults, consistent with regional Niger Delta tectonics. Volumetric analysis indicates STOIIP of 6,090, 4,381 and 5,658 ($\times 10^3$ bbl) for reservoir sand I, II and III respectively. On this basis, reservoir A is the prospective hydrocarbon target in the field, reservoir III is the second most prospective, and reservoir sand II is the least prospective of the three reservoirs.

5.0 References

Anthony, O. O., Ogie, M. E., & Emmanuel, E. O. (2018). Petrophysical evaluation of Otebe Field, onshore Niger Delta, Nigeria. International Journal of Research and Innovation in Applied Science, 3(11).

Asquith, G., & Krygowski, D. (2004). Basic well log analysis (2nd ed.). AAPG Methods in Exploration Series 16.

Doust, H., & Omatsola, E. (1989). Niger Delta. AAPG Bulletin, 48, 201–238.

Doust, H., & Omatsola, E. (1990). “Niger Delta”, In: Edwards, J. D., and Santogrossi,

Doust, H., & Omatsola, E. (1990). Niger Delta. In J. D. Edwards & P. A. Santogrossi (Eds.), Divergent/Passive Margin Basins (AAPG Memoir 48, pp. 239–248). AAPG.

Edem, P. A., Obi, D. A., Ugar, S. I., Obasi, M. E., Mbange, C. E. (2026). Stratigraphic trap Configurations, Seismic Sequence and Facies Analysis of the ‘Ekwai’ Field: Implications for hydrocarbon Exploration In the Niger Delta. Communication in Physical Sciences 13(7): 1188-1213.

Emujakporue, G. O., & Ngwueke, M. I. (2013). Structural interpretation of seismic data from an XY field, onshore Niger Delta, Nigeria. Journal of Applied Science and Environmental Management, 17, 153–158.

Evamy, B. D., Haremboure, J., Kamerling, P., Knaap, W. A., Molloy, F. A., & Rowlands, P. H. (1978). Hydrocarbon habitat of Tertiary Niger Delta. AAPG Bulletin, 62, 1–39.

Hartman, R. A., & Beaumont, E. A. (1999). Predicting reservoir system quality and performance. In E. A. Beaumont & N. H. Foster (Eds.), Exploring for Oil and Gas Traps (AAPG Treatise of Petroleum Geology).

Levorsen, A. H. (1967). Geology of petroleum (2nd ed.). W. H. Freeman.

Nwajide, C. S. (2013). *Geology of Nigeria's sedimentary basins*. Lagos: CSS Bookshops Ltd.

of Petroleum Geologists Memoir, 48, 239-248

Onyia, E. C., Selley, R. C., & Adeoti, L. (2002). Structural styles in the Niger Delta petroleum province. Nigerian Association of Petroleum Explorationists Bulletin, 15, 34–45.

P.A., Editions, Divergent/Passive Margin Basins: Tulsa, American Association

Schlumberger. (1974). Log interpretation manual. Schlumberger Educational Services, Houston.

Short, K. C., & Stauble, A. J. (1967). Outline of geology of Niger Delta. AAPG Bulletin, 51, 761–779.

Tuttle, M. L. W., Charpentier, R. R., & Brownfield, M. E. (1999). The Niger Delta petroleum system: Niger Delta province, Nigeria, Cameroon, and Equatorial Guinea, Africa (USGS Open-File Report 99-50-H). U.S. Geological Survey.

Statement and Declarations

Competing Interests

The authors declared no competing interests

Ethical Consideration

Not applicable

Funding

The authors declared no external source of funding

Availability of data and material

All data used in this manuscript are original except those duly acknowledged and cited by the author.

Author Contribution

P.A.E. conceived the study, interpreted the seismic and petrophysical data, and drafted the manuscript. S.I.U. supervised the research and critically revised the manuscript. S.U.E. contributed to data analysis and literature review. D.A.O. supported reservoir characterization and interpretation. C.E.M. assisted with volumetric reserve estimation and visualization. M.E.O. performed data validation, edited the manuscript, and approved the final version.